CAINE 1996, pp 115-120. ISCA, Orlando FL, Dec. 1996

Modeling of Vehicle Dynamics using Matrix-Vector Oriented Calculation in Matlab.

G. Edzko Smid, Ka C. Cheok and K. Kobayashi
Department of Electrical and Systems Engineering
School of Engineering and Computer Science
Oakland University Rochester, MI 48309-4401

Abstract

Modeling of a 19-degree of freedom, 4-wheel vehicle dynamics is presented. The equations of the model hold for suspension, tire slip, wheel and body dynamics of the vehicle. Attention was given to the matrix-vector oriented calculations in MATLAB[1]. This approach results in a more efficient simulation program that runs much faster and reads more clearly than programs without it. Moreover, the compact matrix-vector model can readily be extended to include the dynamics of additional wheels for the vehicle by simply increasing the size of appropriate matrices in the equations. The equations were tested using a high performance graphic computer. Application of the simulation is also discussed

Keywords: Modeling, Vehicle Dynamics, Simulation, Matrix-vector calculation.

1 Introduction

This paper explains a 19-degree of freedom dynamics model of a vehicle. The model is a useful aid in the research of antilock brake systems, traction control systems and active suspension. The simulation was used to gain more knowledge about the dynamical behaviour and handling of a vehicle in different environments.

The model represents the dynamics of the car body (6 degrees of freedom), wheel suspension hops (4 d-o-f), wheel spin (4 d-o-f), wheel camber angle (4 d-o-f) and frontwheel steering (1 d-o-f). It holds for second order suspension dynamics with detailed equations for motion between the body and the wheels. The slip-dynamics are implemented using the Dugoff tire model [1].

This paper capitalizes the efficient math operators in MATLAB. When programmed appropriately, its built-in vector and matrix operations are more than an order of magnitude faster than its compiler/interpreter operations [3]. Another advantage lies in the fact that the dynamics of all the wheels can be grouped into single equations. This makes the math code more compact and easier to understand. Furthermore the matrix coding allows it to be extended to multi axle vehicles, that have a single body.

[1] MATLAB is a High-Performance Numeric Computation and Visualization Software package of the MathWorks, Inc.

2 Notations

To define the vehicle kinematics, six reference frames were employed: an inertial reference frame $\mathcal{N}$, a body fixed reference frame $\mathcal{A}$ and four wheel fixed reference frames $\mathcal{T}_1$, $\mathcal{T}_2$, $\mathcal{T}_3$ and $\mathcal{T}_4$. The inertial coordinate system is based on the **SAE** standard. The body fixed coordinate system has its origin at the vehicle center of gravity. The x body axis points forward and forms the roll axis of the vehicle; the y axis points to the right and forms the pitch axis and the z direction points downwards and forms the yaw axis of the vehicle body. Roll pitch and yaw will further on be denoted by ϕ, θ and ψ respectively.
To explain vectors and matrices we adopt the following notation. A matrix or vector will always be boldface and the indices will mean ${}^{to}\boldsymbol{M}_{frame}$. For instance a transformation of a vector from the inertial to the body frame is as follows

$$ {}^{\mathcal{N}}\boldsymbol{X} = R_z R_y R_x \, {}^{\mathcal{A}}\boldsymbol{X} \; = \; {}^{\mathcal{N}}R_A \, {}^{\mathcal{A}}\boldsymbol{X}. \qquad (1) $$

In addition, some special syntax of matrix/vector operations for MATLAB has to be mentioned. 1) Addition/subtraction of a matrix with a scalar means that the scalar is applied to each element in the matrix. 2) The `.*` operation stands for the element-wise multiplication of two matrices rather than the matrix multiplication. 3) Boolean logic and standard arithmetic can be expressed in a single equation.

3 Model

We consulted various references, including [6] in deriving the dynamics of the vehicle. We will present

Symbol	Size	Physical interpretation	units
A, B, C	3×4	Geometry locations of spring-body anchor, spring-wheel anchors and tire-ground contact points	m
T_B	3×1	Torques about body (ϕ,θ,ψ)	Nm
v	3×1	Velocity of the body C.G. (x, y, z directions)	m/s
P	3×1	Position of the body C.G. (x, y, z directions)	m
$\mathbf{\Omega}$	3×1	Gyroscopic angular velocity of body (ω_x,ω_y,ω_z)	rad/s
$\tilde{\mathbf{\Omega}}$	3×1	Euler transformed angular body velocities ($\dot{\phi}$,$\dot{\theta}$,$\dot{\psi}$)	rad/s
ω_W	1×4	Spin velocities of the wheels (FR FL RR RL)	rad/s
F_S	3×4	Spring deflection forces (x,y,z $\times$ each spring)	N
F_T	1×4	Tire deflection forces	N
F_D	3×4	Slip forces on wheels	N
F_W	1×4	Total forces on the weels	N
T_W	1×4	Torques about wheel axels	Nm
δ_T	1×4	Tire deflections	m
δ_S	1×4	Spring deflections	m
$\hat{\delta}_S$	1×4	Spring deflections from equilibrium	m
S_W	1×4	Spinning speed of the wheel	m/s
I	3×1	Inertia vector for the body	kgm/s

Table 1: The symbols and their physical meaning

a summary of the matrix/vector equations which were used for the MATLAB simulation. The main matrices and vectors used for the model are defined in Table 1.

3.1 Suspension

Knowing the position and angular rotations of the vehicle body and assuming that the wheels touch the ground, the spring lengths $\boldsymbol{\delta}_S$ can be derived as follows. The anchor point of the spring to the body is denoted by $\boldsymbol{A}$. $\boldsymbol{A} = [\boldsymbol{A_1}\ \boldsymbol{A_2}\ \boldsymbol{A_3}\ \boldsymbol{A_4}]$ where $\boldsymbol{A}_i = [A_{i,x}\ A_{i,y}\ A_{i,z}]'$ points to the location of the i-th anchor. They are part of the geometry of the body and therefore known within the body frame, i.e., ${}^{\mathcal{A}}\boldsymbol{A}_i$ is fixed. We can use the transformation ${}^{\mathcal{N}}R_{\mathcal{A}}$ and take the z-coordinate to derive the height of the anchors above ground with respect to the inertial frame. That is, ${}^{\mathcal{N}}\boldsymbol{A}_z$ is the third row of the 3×4 matrix ${}^{\mathcal{N}}\boldsymbol{A} = {}^{\mathcal{A}}\boldsymbol{R}_{\mathcal{N}}\ {}^{\mathcal{A}}\boldsymbol{A} + {}^{\mathcal{N}}\boldsymbol{P}$. The height of the spring-wheel anchor $\boldsymbol{B}$ will have a height of the maximum tire radius $\boldsymbol{R}_{max}$ minus the tire deflections $\boldsymbol{\delta}_T$. In Figure 1 shows the difference in vertical height between the two anchor points $\boldsymbol{A}$ and $\boldsymbol{B}$ which is the difference in the z-coordinates in the N-frame.

It is assumed that the suspension deflections are in the z-direction of frame $\mathcal{A}$. The unit vector in this direction will be ${}^{\mathcal{A}}\bar{n} = [0, 0, 1]'$ and can be transformed to the inertial frame as ${}^{N}\bar{n} = {}^{\mathcal{N}}R_{\mathcal{A}}\ {}^{A}\bar{n}$.

From geometry it can be shown that the spring deflection is given by

$$\boldsymbol{\delta}_S = \left| {}^{\bar{N}}\bar{n} \frac{{}^{\mathcal{N}}\boldsymbol{A}_z - gnd - \boldsymbol{R}_{max} + \boldsymbol{\delta}_T}{{}^{\mathcal{N}}\bar{n}_z} \right|. \qquad (2)$$

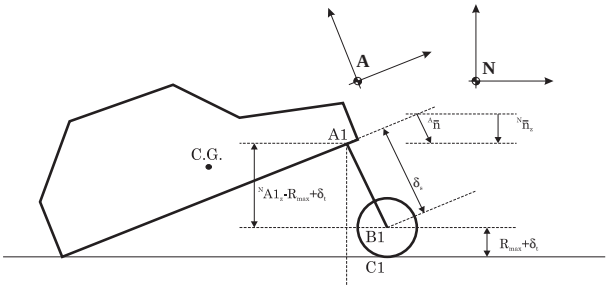

Figure 1: Visual representation of the derivation of the spring deflections

where gnd is a 1×4 vector that holds the ground altitude at the four tire-contact locations. From the above deflections we can derive the spring displacement from equilibrium to be $\hat{\boldsymbol{\delta}}_S = \boldsymbol{D}_S - \boldsymbol{\delta}_S$, where $\boldsymbol{D}_S$ denotes the spring extension when the vehicle is in equilibrium. The deflection rate is its derivative

$$\dot{\hat{\boldsymbol{\delta}}}_S = \frac{\hat{\boldsymbol{\delta}}_{S,k} - \hat{\boldsymbol{\delta}}_{S,k-1}}{\Delta t} \qquad (3)$$

where k is the current iteration step and Δt stands for the integration step size.

An additional force on the suspension called antiroll is introduced by the mechanical design of the vehicle to produce a counter torque when there is a roll of the vehicle. This torque will be modeled here as an additional force at the suspension locations. The force is basically derived as a left and right suspension differential from (2), divided by the track width, which is a geometric constant, and then multiplied by an equivalent roll stiffness coefficient. This is written in formula

as

$$\boldsymbol{F}_{roll} = K_{roll}\frac{\boldsymbol{\delta}_{S,left} - \boldsymbol{\delta}_{S,right}}{TW}. \quad (4)$$

where TW stands for the track width of the car. The spring forces are due to the deflection and the deflection rate, proportional to respectively the spring constant K_s and the damper constant B_s and the equivalent roll stiffness as given in (4). They become

$${}^{\mathcal{A}}\boldsymbol{F}_{S,z} = \hat{\boldsymbol{\delta}}K_s + \dot{\hat{\boldsymbol{\delta}}}B_s + \boldsymbol{F}_{roll}. \quad (5)$$

and act only in the z-direction with reference to the body frame. By assumption, ${}^{\mathcal{A}}\boldsymbol{F}_S = [0\ 0\ {}^{\mathcal{A}}\boldsymbol{F}_{S,z}]'$.

3.2 Tire Slip Forces

A slip model derived by Dugoff [1] will be applied for deriving the shear forces which are caused by the slip of the road-tire contact patch. The Dugoff model needs two states to be derived and several parameters to calibrate the resulting shear forces. The result of the model will be two normalized forces in the longitudinal and lateral direction respectively, with respect to the tire frames. The traction shear forces on the tire carcass can be derived by multiplying these normalized values with the normal force $|{}^{\mathcal{N}}\boldsymbol{F}_z|$ between the tire and road. ${}^{\mathcal{N}}\boldsymbol{F}_z$ is the reaction force of the tire deflection forces $\boldsymbol{F}_W$ that will be explained in Section 3.3.2.
The states for the model will be the spatial travel of the tire, transformed to the tire frame $\mathcal{T}$ and the patch travel caused by spin velocity of the wheel $\boldsymbol{\omega}_W$. The cross-product of the yaw-rate $\dot{\psi}$ and the vectors from the C.G. to the centers of the road-tire contact patches, will derive the translation of the contact patch, caused by change of heading of the vehicle. Since we assume a horizontal flat ground surface, only the x and y information in this product is of interest, the anchor location matrix $\boldsymbol{A}$ is used with zero values for the $\boldsymbol{z}$ coordinate. It is denoted by $\boldsymbol{A}_{x,y}$. The wheel travel is calculated by adding this translation to the vehicle velocity ${}^{\mathcal{N}}\boldsymbol{v}$ and then transforming this result to the tire frame. In formula this is written as follows.

$$\begin{aligned} {}^{\mathcal{T}}\boldsymbol{v} &= {}^{\mathcal{T}}R_{\mathcal{A}}\,({}^{\mathcal{A}}R_{\mathcal{N}}\,{}^{\mathcal{N}}\boldsymbol{v} + \dot{\boldsymbol{\psi}} \times \boldsymbol{A}_{x,y}) \text{ for front wheels} \\ &= {}^{\mathcal{A}}R_{\mathcal{N}}\,{}^{N}\boldsymbol{v} + \dot{\boldsymbol{\psi}} \times \boldsymbol{A}_{x,y} \text{ for rear wheels} \end{aligned} \quad (6)$$

For the rear tires we do not transform from $\boldsymbol{A}$ to T because the frames of the rear wheels and the body are fixed parallel. Note that (6) is a combined vector/matrix operation that results in a 3×1 vector which holds the velocity of the wheel in longitudinal, lateral and vertical directions respectively.
To estimate the amount of slip, caused by just the wheel spin velocity, the angular spin velocity will be transferred to a linear speed, by multiplying with the effective tire radius as $\boldsymbol{S}_W = \boldsymbol{\omega}_W(\boldsymbol{R}_{max} - \boldsymbol{\delta}_T)$.
Since the angle of the slip vector, caused by the wheel spin will always be zero with respect to $\mathcal{T}$, the total angle of slip is just the angle of the spacial wheel travel. It can be written as the tangent of the amount of lateral over longitudinal slip:

$$\boldsymbol{\alpha}_s = \arctan\left(\frac{|{}^{\mathcal{T}}\boldsymbol{v}_y|}{|{}^{\mathcal{T}}\boldsymbol{v}_x|}\right) \quad (7)$$

The slip-ratio is introduced as a normalized number to indicate the amount and direction of slip. It ranges from -1 to 1 and will be calculated as

$$\boldsymbol{r}_s = \frac{\boldsymbol{S}_W - \boldsymbol{v}_x}{\max({}^{\mathcal{T}}\boldsymbol{v}_x, \boldsymbol{S}_W)} \quad (8)$$

From the Dugoff tire model, the following equations

Sym	name	Units
C_α	Cornering stiffness	N
C_s	Longitudinal stiffness	N
μ_0	Nominal friction coefficient	
A_s	Friction reduction	sec/m

Table 2: Typical Parameters for the Tire Mechanical Characteristics.

are applied to transfer the slip-ratio (8) and the slip angle (7) into the longitudinal and the lateral slip respectively

$$\boldsymbol{F}_{\text{lon}} = \begin{cases} \dfrac{C_s\ \boldsymbol{r}_s}{1-\boldsymbol{r}_s} & \bar{\boldsymbol{s}}_R < 0.5 \\ \dfrac{C_s\ \boldsymbol{r}_s}{(1-\boldsymbol{r}_s)\bar{\boldsymbol{s}}_R}\left(1 - \dfrac{1}{4\bar{\boldsymbol{s}}_R}\right) & \bar{\boldsymbol{s}}_R \geq 0.5 \end{cases} \quad (9)$$

$$\boldsymbol{F}_{\text{lat}} = \begin{cases} \dfrac{C_\alpha \tan(\boldsymbol{\alpha}_s)}{1-\boldsymbol{r}_s} & \bar{\boldsymbol{s}}_R < 0.5 \\ \dfrac{C_\alpha \tan(\boldsymbol{\alpha}_s)}{(1-\boldsymbol{r}_s)\bar{\boldsymbol{s}}_R}\left(1 - \dfrac{1}{4\bar{\boldsymbol{s}}_R}\right) & \bar{\boldsymbol{s}}_R \geq 0.5 \end{cases} \quad (10)$$

Here $\bar{\boldsymbol{s}}_R$ is an auxiliary variables which is calculated as

$$\bar{\boldsymbol{s}}_R = \frac{1}{\mu|{}^{\mathcal{N}}\boldsymbol{F}_z|(1-\boldsymbol{r}_s)}\sqrt{C_s^2\boldsymbol{r}_s^2 + C_\alpha^2\tan^2\boldsymbol{\alpha}_s}. \quad (11)$$

where μ is defined by

$$\mu = \mu_0\left(1 - A_s\ {}^{\mathcal{T}}\boldsymbol{v}_x\sqrt{\boldsymbol{r}_s^2 + \tan^2\boldsymbol{\alpha}_s}\right) \quad (12)$$

The equations are explained in more detail in [1]. The slip forces are then combined in a vector with only x- and y-entries as

$${}^{\mathcal{T}}\boldsymbol{F}_D = \begin{pmatrix} \boldsymbol{F}_{\text{lon}} \\ \boldsymbol{F}_{\text{lat}} \\ 0 \end{pmatrix}. \quad (13)$$

This vector can then be transformed from tire frame to body frame as ${}^{\mathcal{A}}\boldsymbol{F}_D = {}^{\mathcal{A}}R_{\mathcal{T}}\,{}^{\mathcal{T}}\boldsymbol{F}_D$.

3.3 Wheel Equations of Motion

The wheel dynamics can be separated into angular motion about the y-axis in the wheel frame $\mathcal{T}$ and height with respect to ground level. Also a derivation of the camber angle will be given and steering compliance will be discussed.

3.3.1 Wheel spin dynamics

The longitudinal slip force, the driving torque and the brake torque account for the resulting wheel spin accelerations. They can be written as

$$\begin{aligned} {}^{\mathcal{T}}\boldsymbol{T}_D = {} & {}^{\mathcal{T}}\boldsymbol{F}_{\text{lon}}(\boldsymbol{R}_{max} - \boldsymbol{\delta}_T) \\ & + KTQ(VC - {}^{\mathcal{T}}\boldsymbol{v}_x)\ ({}^{\mathcal{T}}\boldsymbol{v}_x < VC\ \&\ VC > 0) \\ & + \boldsymbol{\omega}_W\ tqb \end{aligned}$$

where VC is the command velocity, KTQ is the drive torque constant and tqb is the brake torque, applied by the driver. Since this model assumes front wheel drive, the traction torque in the second term only applies to the front wheels.
Now the wheel spin accelerations can be derived by dividing the wheel torque by the inertia

$$\ddot{\boldsymbol{\omega}}_W = \frac{{}^{\mathcal{T}}\boldsymbol{T}_D}{\boldsymbol{I}_{ww}}. \tag{14}$$

where $\boldsymbol{I}_{ww}$ is the moment of inertia associated with the wheel spin. The actual wheel spin velocities are calculated by integrating the accelerations.

3.3.2 Wheel deflection dynamics

The forces on the tires that causes them to deflect are assumed to be the same as the forces that of the springs, in the z-direction in $\mathcal{A}$. The inflated tire is modeled as a spring and a damper system which yields

$$\boldsymbol{F}_T = \boldsymbol{\delta}_T K_w + \dot{\boldsymbol{\delta}}_T B_w \tag{15}$$

where K_w and B_w are respectively the stiffness and damping effect of the rubber. The forces acting on the wheels are from the springs, the tire deflection and the gravity.

$${}^{\mathcal{N}}\boldsymbol{F}_W = {}^{\mathcal{N}}R_{\mathcal{A}}\ {}^{\mathcal{A}}\boldsymbol{F}_S - \boldsymbol{F}_T + MT\ G \tag{16}$$

where MT is the mass of the wheel and G stands for the gravitational acceleration. Deflection accelerations can be calculated by dividing (16) by MT. Deflection rates and deflections can then be derived by integration. The normal force ${}^{\mathcal{N}}\boldsymbol{F}_z$ is the opposite of these tire deflection forces.

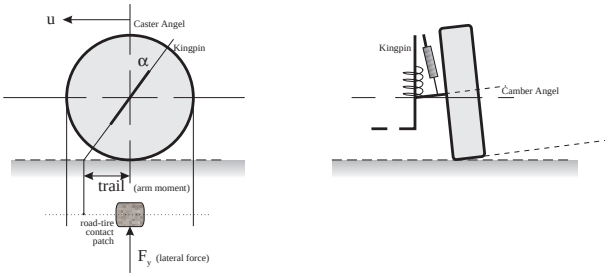

Figure 2: The Steering Compliance is modeled according to the diagram on the left hand side. The Caster angle can be derived with the digram on the right hand side.

3.3.3 Camber angle

The Camber angle of the wheel can be viewed upon as the roll, caused by the lateral force with respect the wheel frame $\mathcal{T}$. The lateral force is caused by the slip, and given in (9) and (10). Figure 2 shows the camber angle in the right diagram. The dynamic equation for the camber angle is given by

$$J_{kp}\ddot{\boldsymbol{\theta}}_c + B_c\dot{\boldsymbol{\theta}}_c + K_c\boldsymbol{\theta}_c = \boldsymbol{F}_{\text{lat}\cdot} * (\boldsymbol{R}_{max} - \boldsymbol{\delta}_T) \tag{17}$$

where J_{kp} stands for the inertia moment of the wheel about the kingpin axis, $\boldsymbol{\theta}_c$ holds the camber angle, $(\boldsymbol{R}_{max} - \boldsymbol{\delta}_T)$ represents the effective tire radius, B_c is the damping effect and K_c is the equivalent stiffness coefficient of the connecting system. A simplification without dynamics is given by

$$\boldsymbol{\theta}_c = \frac{\boldsymbol{F}_{\text{lat}\cdot} * (\boldsymbol{R}_{max} - \boldsymbol{\delta}_T)}{K_c} \tag{18}$$

3.3.4 Steering Compliance

The model for the steering compliance has been adapted from [2]. The angle α between the kingpin and the normal unit vector in the z-direction is referred to as the *Caster angle*. The distance between the center of the tire contact patch and the point where the axis of the kingpin intersects with the road surface will be called the AA. This is shown in the left of Figure 2. The moment M_{ss} about the kingpin, caused by the lateral force on the wheel can be written as

$$M_{ss} = \boldsymbol{F}_{\text{lat}}\xi\cos(\alpha) \tag{19}$$

where ξ is the $trail$, shown in Figure 2. The dynamic equation for the steered wheel, is given by

$$\begin{aligned} & J_{kp}\frac{\ddot{\theta}_w}{N_G} + B_{st}\frac{\dot{\theta}_w}{N_G} + K_{st}\frac{\theta_w}{N_G} = \\ & K_{st}\theta_{cmd} + B_{st}\dot{\theta}_{cmd} - M_{ss} \end{aligned} \tag{20}$$

where J_{kp} stands for the inertia moment of the wheel about the kingpin axis, θ_w is the angle of the steered

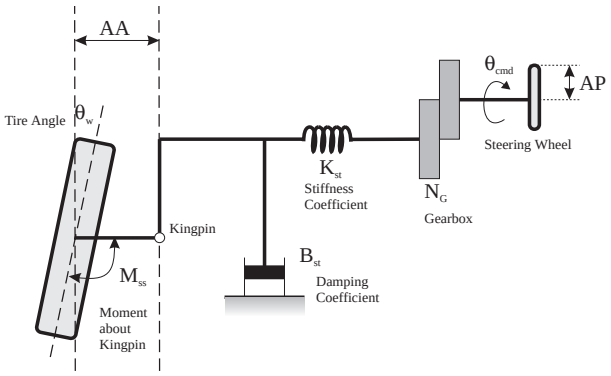

Figure 3: The second order steering system model

wheel, N_G stands for the gear box ratio of the steering system, B_{st} is the equivalent damping coefficient and K_{st} the equivalent stiffness coefficient of the steering system. θ_{cmd} is the angle of the steering wheel. This model of the steering system is drawn in Figure 3. A simplified model that contains no dynamics will give the angle of the steered wheel from the steering wheel angle as follows :

$$\theta_w = N_G \left(\theta_{cmd} - \frac{\boldsymbol{F}_{\text{lat}} M_{ss}}{K_{st}} \right). \tag{21}$$

3.4 Vehicle body Equations of Motion

The vehicle body has freedom of motion in all angular and cartesian directions. First the rotational dynamics will be discussed and than the spacial dynamics.

3.4.1 Rotational Dynamics

Torques are due to forward and side slip forces at the tire-road contact points and the spring forces acting at the anchor locations. Torques by slip are calculated by taking the cross product of ${}^{A}F_D$ and the vectors of the tire-road contact points to the body center of gravity. Torques caused by the suspension are derived with the cross product of the body-spring anchor locations and ${}^{A}F_S$ which only have a z-component in A. In formula

$$\boldsymbol{T}_B = \sum_{wheels} (\boldsymbol{A} \times {}^{\mathcal{A}}\boldsymbol{F}_S) + \boldsymbol{C} \times {}^{\mathcal{A}}\boldsymbol{F}_D) \tag{22}$$

In (22), $\boldsymbol{C}$ stands for the vectors from the body C.G. to the road-tire contact points and $\boldsymbol{A}$ from C.G. to spring-body anchors. See Figure 1.
The angular body accelerations are calculated by subtracting the inertial accelerations from the torques and then dividing by the inertias as

$$\dot{\boldsymbol{\Omega}} = (\boldsymbol{T}_B - \boldsymbol{\Omega} \times (\boldsymbol{I} .* \boldsymbol{\Omega}))(\boldsymbol{I})^{-1} \tag{23}$$

Integration yields the next value for $\boldsymbol{\Omega}$.
These angular velocities are instantaneously derived from the rotational accelerations. If we want to derive the roll, pitch an yaw, being the separated angles about the different body axes, the angular velocities have to be transformed into Euler angle rates, as

$$\tilde{\boldsymbol{\Omega}} = \begin{pmatrix} 1 & sin(\phi)tan(\theta) & cos(\phi)tan(\theta) \\ 0 & cos(\phi) & -sin(\phi) \\ 0 & sin(\phi)sec(\theta) & cos(\phi)sec(\theta) \end{pmatrix} \Omega. \tag{24}$$

Again, integration yields the orientation vector with roll, pitch and yaw (ϕ, θ, ψ).

3.4.2 Translational Dynamics

For the spatial motion of the vehicle body, the acting forces are divided by the appropriate masses to derive the accelerations. The forces are caused by the springs, slip and gravity. The body acceleration becomes then

$$\ddot{\boldsymbol{P}} = \begin{pmatrix} {}^{\mathcal{N}}R_{\mathcal{A}} \sum\limits_{springs} {}^{\mathcal{A}}\boldsymbol{F}_S \\ \hline M \end{pmatrix} \tag{25}$$

$$+ \begin{pmatrix} {}^{\mathcal{N}}R_{\mathcal{A}} \sum\limits_{tires} {}^{\mathcal{A}}\boldsymbol{F}_W \\ \hline M + 4MT \end{pmatrix} \tag{26}$$

$$+ G \tag{27}$$

where M is the mass of the car and $G = [0\ 0\ 9.81]'$ is the gravity vector. The velocities and positions can be derived from the accelerations by integration.

4 Implementation

The vehicle model has been implemented in MATLAB and also in EASY5. In Matlab the model is implemented using scripts that exploit the matrix-vector calculus capabilities. Since MATLAB is a prototyping simulation software that has an interpretive execution structure, the mathematical section of the simulation runs approximately 4 times slower than real-time, when executed on a SGI Max Impact workstation, (250 MHz and with a R4400 processor). A sampling time of 10 ms was used in the simulation. The Max Impact is about three times faster than a 90 MHz Pentium computer.

The model was also evaluated using different software. Figure 4 shows the implementation in EASY5. The EASY5 Graphical User Interface allows the user to design a structured schematic for the underlying FORTRAN code. Running on an SGI ONYX 4-cpu workstation, the simulation ran about 150% faster than real-time, using a sampling time of 1 ms.

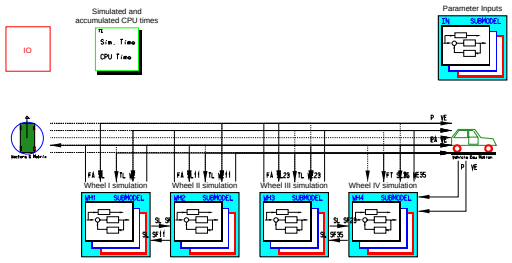

Figure 4: Main Schematic of the vehicle model as is implemented in Easy 5, based on the Matrix-Vector Matlab formulation.

5 Applications

Applications of real-time simulation can be found in research on traction control and antilock brake systems with hardware in the loop simulations [4]. Road surface and tire characteristics in the software can be changed on the fly. This saves both time and test-track facilities and resources.

Real-time simulation has also been combined with animation and a driver cab, where a human driver can control a virtual vehicle, driving through a fictional scenery. In this fashion research can be done on human behaviour in various simulated dangerous situations, without putting the driver at risk. The simulator can also be used to train and improve the driver's skill with advanced driver-aid devices as active suspension and ABS. Simulations of automobile maneuvers have been performed before on digital machines, using a simpler model [5].

For the different research objectives, output can be in the form of curves and plots, an animated wire-model of a vehicle, a scenery with real-time animation of a sophisticated model and even, as mentioned a driver cab.

6 Conclusions

The model presented in this paper contributes mainly in the area of research to vehicle dynamics and behaviour. The compactness of the calculus allows real-time implementation and enables research into advanced areas. Applications show the need and usefulness of the model.

Simulations in general decrease costs and increase efficiency and safety of tests. It also allows testing of abnormal and extreme scenarios without months of preparation or expensive facilities.
Furthermore it allows to demonstrate in a comfortable environment the implementation of various advanced driving-aid devices.

References

[1] Howerd Dugoff, P. S. Fancher, and Leonard Segel. An analysis of tire traction properties and their influence on vehicle dynamic performance. *SAE Paper No.700377*, pages 341–365, 1970.

[2] Y. Hossam El-Deen and Ali Seireg. Mechatronics for cars: Integrating machines and electronics to prevent skidding on icy roads. *Computers in Mechanical Engineering*, pages 10–22, January 1987.

[3] J. Little, C. Moler, and The MathWorks Inc. *MATLAB High-Performance Numeric Computation and Visualization Software*. The MathWorks Inc., August 1992.

[4] Larry Michaels. The use of a graphical modeling environment for real-time hardware-in-the-loop simulation of automotive abs systems. SAE Paper No.930507. pages 29-32.

[5] Brian Mitchell, Robert Abrams, and Richard A. Scott. All-digital simulation of simple automobile maneuvrers. *SIMULATION*, pages 179–186, December 1981.

[6] Author Unknown. Real-time, seventeen-degree-of-freedom motor vehicle simulation. Technical report, Applied Dynamics International, Copyright 1989,1990,1995.